



## Shape-based virtual screening, synthesis and evaluation of novel pyrrolone derivatives as antiviral agents against HCV



Marcella Bassetto <sup>a,\*</sup>, Pieter Leyssen <sup>b</sup>, Johan Neyts <sup>b</sup>, Mark M. Yerukhimovich <sup>c</sup>, David N. Frick <sup>c</sup>, Andrea Brancale <sup>a</sup>

<sup>a</sup> Cardiff School of Pharmacy and Pharmaceutical Sciences, Cardiff, King Edward VII Avenue, Cardiff CF103NB, UK

<sup>b</sup> Rega Institute for Medical Research, University of Leuven, Belgium

<sup>c</sup> Department of Chemistry & Biochemistry, University of Wisconsin-Milwaukee, Milwaukee, Wisconsin 53211, United States

### ARTICLE INFO

#### Article history:

Received 25 November 2016

Revised 30 December 2016

Accepted 31 December 2016

Available online 3 January 2017

#### Keywords:

Ligand-based virtual screening

Shape-similarity search

Novel pyrrolones

Anti-HCV activity

### ABSTRACT

A ligand-based approach was applied to screen *in silico* a library of commercially available compounds, with the aim to find novel inhibitors of the HCV replication starting from the study of the viral NS3 helicase. Six structures were selected for evaluation in the HCV subgenomic replicon assay and one hit was found to inhibit the HCV replicon replication in the low micromolar range. A small series of new pyrrolone compounds was designed and synthesised, and novel structures were identified with improved antiviral activity.

© 2017 Elsevier Ltd. All rights reserved.

Hepatitis C virus (HCV) is a major cause of chronic liver disease and affected individuals are at high risk of developing hepatic steatosis, fibrosis, cirrhosis and hepatocellular carcinoma.<sup>1</sup> There is no vaccine available to prevent the infection and such vaccine is not soon expected. The standard of care used to be a combination of pegylated interferon (pegIFN) and ribavirin, a therapy not specific for HCV and efficient in 50% of treated patients, with many associated side effects.<sup>2</sup> However, new interferon-free combinations of direct acting antivirals (DAAs) have revolutionized HCV prognosis and treatment.

HCV ~9000 nt single-stranded, positive-sense RNA genome encodes six non-structural proteins (NS2, NS3, NS4A, NS4B, NS5A and NS5B) essential for virus replication.<sup>3</sup> Oral combination treatment regimens with NS5B polymerase, NS3 protease and/or NS5A inhibitors have become the standard of HCV care,<sup>4–8</sup> but they are associated with the development of resistant mutants<sup>9–13</sup> and high costs.<sup>14,15</sup> Due to these limitations, the development of new therapeutics is still needed.

HCV NS3 helicase is one of the most underexploited targets in the search for anti-HCV compounds, with very few specific inhibitors reported so far, none of which reached the clinical stage.<sup>16</sup> The protein main function, essential for viral replication, is the ATP-dependent unwinding of double-stranded RNA sequences.<sup>17–20</sup>

Due to its fundamental role in HCV replication and the lack of inhibitors under development, this enzyme was chosen as target for the computer-aided identification and synthesis of viral replication inhibitors.

A successful computer-based approach for the identification of new biologically active compounds is represented by shape-complementarity search methods.<sup>21</sup> Common docking-based techniques usually estimate the ligand binding energy by a scoring procedure that emphasises electrostatics rather than shape. In ligand-based methods instead, the shapes of known ligands are compared with unknown ones, while the chemical properties of known molecules can be included in the comparison as pharmacophoric or electrostatic models; for these approaches a higher accuracy in finding active compounds has been demonstrated.<sup>22</sup> Ligand-based methods can evaluate two-dimensional similarities, such as fingerprints,<sup>23</sup> or three-dimensional similarities, focusing on the molecule occupational volume. While 2D comparison methods tend to find hits with the same functional groups of the query molecule,<sup>24</sup> 3D search programs such as ROCS focus on the occupational volume associated with each molecule,<sup>25</sup> thus allowing the identification of novel lead structures with a higher level of scaffold diversity.

While previous successful efforts in our research group focused on protein-based approaches for the identification of new antivirals,<sup>26,27</sup> in order to explore the potential of a shape-comparison method in the search for novel anti-HCV agents, this technique

\* Corresponding author.

E-mail address: [bassettom@cardiff.ac.uk](mailto:bassettom@cardiff.ac.uk) (M. Bassetto).

was chosen to screen a library of commercially available compounds. The structures of the dye soluble blue HT **1** and a series of reported compounds derived from **1** were used as starting point,<sup>28</sup> being **1** the only known helicase inhibitor for which a crystal structure in complex with the enzyme is available (PDB ID 1ZJO, Fig. 1).<sup>29</sup>

While **1** is toxic to cells and its effect against the viral replication cannot be evaluated in cell-based assays, several reported HCV NS3 helicase inhibitors have recently been tested in both an optimised enzymatic assay and a replicon cell-based assay.<sup>16</sup> among them, one structural derivative of **1**, triphenylmethane analogue **2** (Fig. 2),<sup>28</sup> has been confirmed to inhibit both the enzyme ( $IC_{50}$  17 ± 7  $\mu$ M) and the viral replication (~80% at 10  $\mu$ M) without relevant cytotoxicity (~75% cell viability at 10  $\mu$ M).<sup>16</sup>

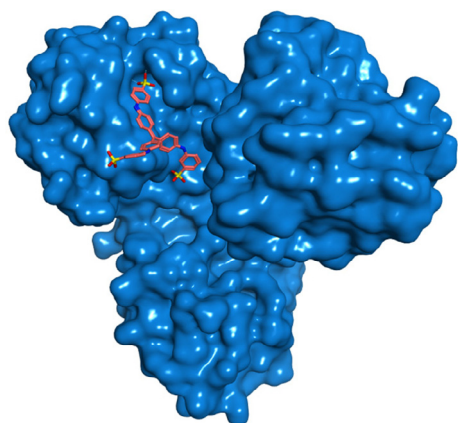


**Figure 1.** Crystal structure of **1** in complex with HCV NS3 helicase (PDB ID 1ZJ0).

Due to its activity profile against the viral replication in cells, **2** was chosen as query for a shape-based screening of the SPECS library<sup>30</sup> using ROCS 3D.<sup>25</sup> In order to evaluate the shape complementarity between the target query and screened compounds, shape-density overlapping volumes of superimposed molecules are considered by the program and scored according to a Tanimoto-like overlapping value. The conformational state of the query molecule plays an essential role for hit selection, since all analysed structures will be scored based on their overlapping with the target conformation. Along with the conformation selection for the query, the evaluation of the different three-dimensional states of the screened structures becomes crucial. First, a conformational search with MOE2015.10 was performed for the creation of a conformational database for the screening compounds.<sup>31</sup> A conformational analysis was also performed on **2**, obtaining multiple low-energy three-dimensional states. The conformational results found for **2** were then compared with the conformation of **1** in the 1ZJ0 crystal structure using MOE2015.10 Flexible Alignment tool.<sup>32</sup> The low-energy conformations found for **2** were rigidly aligned to **1**, and the one corresponding to the best alignment was chosen as query (Fig. 3).

The conformational database obtained for the SPECS compounds was analysed against the selected conformation of **2** with vROCS3.1.2<sup>25</sup> considering both shape and electrostatics complementarity. All screened conformations were ranked based on their similarity score with the given query. A selection was made among the screened molecules to prioritise those with the highest similarity indexes (Combo-shape Tanimoto score) and the biggest number of conformations matching the query. Six compounds were finally selected, purchased and evaluated against the viral replication in a cell-based assay (Supporting Information). Among them, **3a** (Fig. 4) was found to inhibit the viral replication with an EC<sub>50</sub> value of 38  $\mu$ M (Table 1). Its scaffold was chosen for the preparation of a

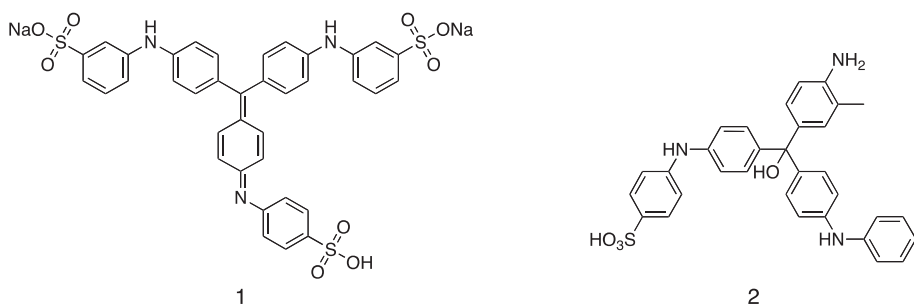


**Figure 2.** Chemical structures of **1** and **2**.

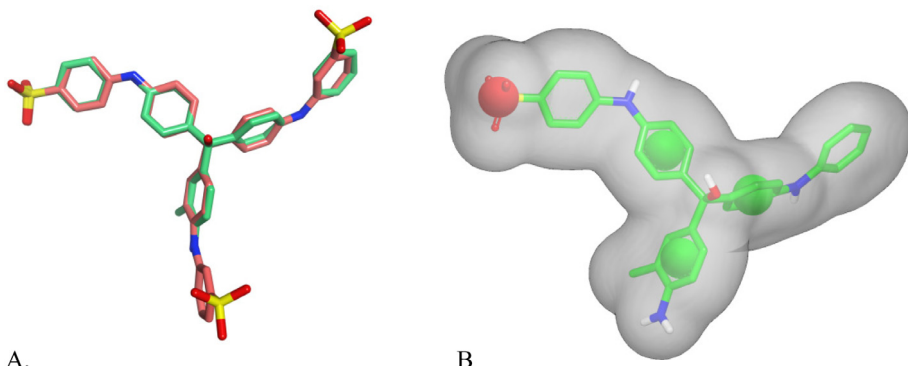


**Figure 3.** (A) Best conformational superimposition between **1**, in pink, and **2**, in green; (B) Query generated from **2** in vROCS3.1.2: the overall molecular shape is represented as grey surface, while the chemical features considered are an H-bond acceptor (red sphere) and three hydrophobic/aromatic centres (green spheres).

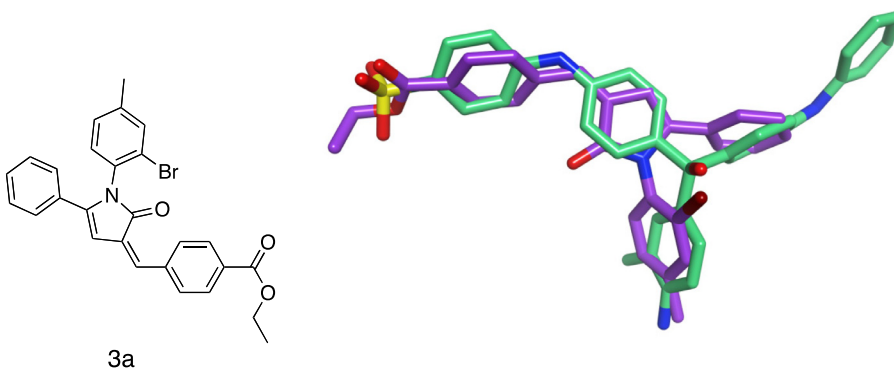


Figure 4. Chemical structure and best alignment found for **3a** (aligned in purple against **2**, in green).

Table 1

Antiviral effect of the test compounds on hepatitis C virus replication in the Huh5-2 replicon system and inhibition of NS3 helicase unwinding activity.

Compound	EC <sub>50</sub> (μM) <sup>a,d,37</sup>	EC <sub>90</sub> (μM) <sup>b,d</sup>	CC <sub>50</sub> (μM) <sup>c,d</sup>	SI <sup>e</sup>	Unwinding IC <sub>50</sub> (μM) <sup>f,16</sup>
<b>3a</b> (SPECS)	38	149	>204	>4	n.d.
<b>3a</b> (synthesised)	20.3 ± 1.1	61.7 ± 2.7	>205	>10	>1000
<b>3b</b>	4.1 ± 2.5	12.4 ± 6.3	>240	>58	>1000
<b>7a</b>	27.2 ± 7.6	100	112	4	>1000
<b>7b</b>	4.7 ± 0.5	14 ± 4.2	30.3 ± 5.9	6.4	>1000
<b>7c</b>	5.9 ± 1.8	21.6 ± 1.8	97.2 ± 8.7	18	438
<b>7d</b>	4.3 ± 1.5	11.6 ± 0.8	25.7 ± 6.4	6	>1000
<b>7e</b>	16.1 ± 2.7	61.7	156 ± 63.3	9.7	>1000
<b>8a</b>	22.5 ± 0.9	81.1 ± 13.1	>244	>11	>1000
<b>9a</b>	43.1 ± 19.9	—	90.8 ± 26.8	2.1	>1000
(VX-950)	0.8 ± 0.2	—	47	58.8	n.d.
Primuline	—	—	—	—	10 ± 2
Aurintricarboxylic Acid	—	—	—	—	0.3 ± 0.1

n.d. Not determined.

<sup>a</sup> EC<sub>50</sub> = 50% effective concentration (concentration at which 50% inhibition of virus replication is observed).

<sup>b</sup> EC<sub>90</sub> = 90% effective concentration (concentration at which 90% inhibition of virus replication is observed).

<sup>c</sup> CC<sub>50</sub> = 50% cytostatic/cytotoxic concentration (concentration at which 50% adverse effect is observed on the host cell).

<sup>d</sup> The EC<sub>50</sub>, EC<sub>90</sub> and CC<sub>50</sub> values are the mean of at least 2 independent experiments, with standard deviations of ±10% of the value quoted unless otherwise stated (mean value ± standard deviations).

<sup>e</sup> SI = the ratio of CC<sub>50</sub> to EC<sub>50</sub>.

<sup>f</sup> Concentration needed to reduce rates of helicase-catalysed DNA unwinding by 50%.

small series of novel derivatives, with which to confirm the biological activity found.

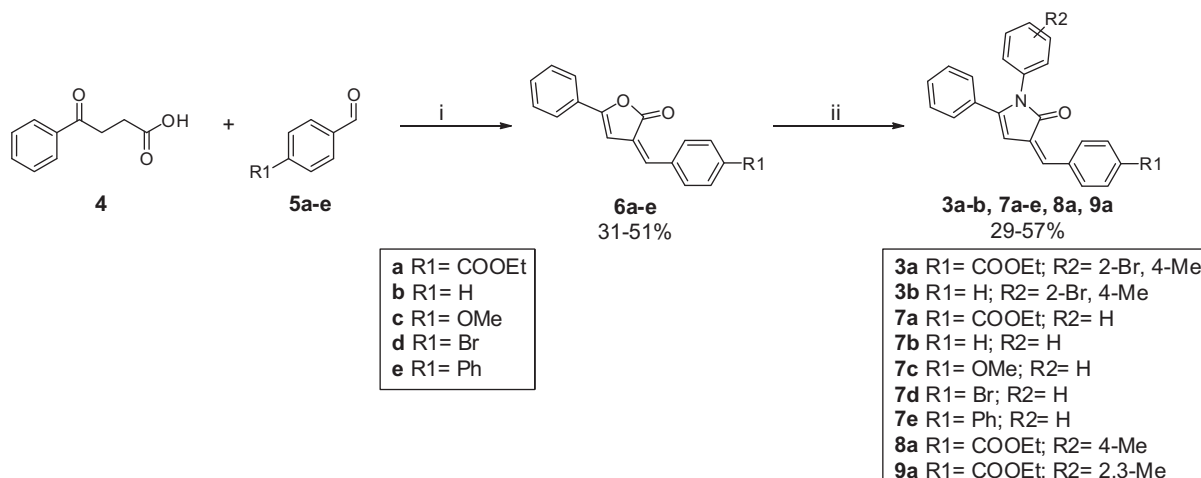
**3a** is characterised by a central pyrrolone nucleus, substituted in position 1 and 5 with two aromatic rings, and linked in position 3 with a phenylidene system. A preliminary series of triphenyl-pyrrolone derivatives was designed by varying the aromatic substituents on the 1-phenyl and 3-phenylidene rings. This small series of compounds was envisaged to confirm the antiviral potential originally found for **3a** and to explore the effect of the aromatic substituents in the two substituted aromatic rings. In particular, removal of the 4-ethyl carboxylate group on the 1-phenyl ring of **3a** was envisaged to confirm its relevance for antiviral activity (**3b**, **7b**), along with its replacement with different electron withdrawing (4-Br in **7d**) and electron donating (4-OMe in **7c** and 4-Phenyl in **7e**) groups. Preliminary modifications designed for the substituted 3-phenylidene ring of **3a** included the removal of both substituents (**7a–e**, **8a**) or of the original 2-Br function only (**8a**), and their replacement with a 2,3-dimethyl substitution (**9a**). All desired compounds were prepared according to an optimised two-step synthetic pathway (Scheme 1).

The strategy carried out began with the condensation of 3-benzoyl propanoic acid **4** with different *para* substituted benzaldehydes **5a–e**, with the formation of butenolide intermediates **6a–e** through furanone ring closure, followed by phenyl-amine displacement of the cyclic ester with the formation of the pyrrolone system in final products **3a–b**, **7a–e**, **8a** and **9**. According to literature pro-

cedures,<sup>33,34</sup> furanone intermediates **6a–e** were obtained by heating the starting materials at 95 °C in acetic anhydride in the presence of sodium acetate. The formation of the central butenolide ring is believed to follow a Perkin condensation between β-benzoylpropionic acid and the substituted aryl aldehyde,<sup>35</sup> which are thought to form an aldol-condensation product that subsequently undergoes internal cyclisation with the formation of the furanone ring. In these conditions only one species, corresponding to the *cis* isomer, is formed.<sup>33</sup> The desired final products were subsequently obtained by treating intermediates **6a–e** with differently substituted anilines, stirring the reaction mixture in glacial acetic acid first at room temperature for 4 h, and then heating to reflux for 22 h. The furanone ring is believed to open as a result of the ammonolysis of the starting compound by the aromatic amine, followed by cyclisation and dehydration events to give the final pyrrolone system.<sup>36</sup>

All newly synthesised pyrrolones were evaluated for their potential antiviral activity in the HCV replicon and cytostatic assay (Table 1).<sup>37</sup> The HCV protease inhibitor telaprevir (VX-950) was included as positive control.

Re-synthesised **3a** confirmed its activity profile, with EC<sub>50</sub>, EC<sub>90</sub> and CC<sub>50</sub> values close to the ones previously found for the batch acquired from SPECS. The presence of an ethyl ester function in the 3-phenylidene ring does not appear to be essential for activity retention, since **3b**, where this group is removed, is the most active analogue found so far. A similar profile can be identified for



**Scheme 1.** Reagents and conditions: (i) AcONa, Ac<sub>2</sub>O, 95 °C, 2 h; (ii) Substituted aniline, AcOH, rt, 4 h, reflux, 22 h.

derivatives **7b–e**, where the 1-phenyl ring is unsubstituted and the ethyl ester group is replaced respectively with 4-H, 4-Me, 4-Br and 4-phenyl groups. For analogues **7b–d** however an increased cytotoxic effect can also be observed. Activity retention found for **7a** and **8a** seems to indicate that also the presence of the 2-bromo, 4-methyl substituent in the 1-phenyl ring is not essential for antiviral activity, while the insertion of a methyl group in position 3 of this ring and the replacement of the original 2-bromo substituent with an extra methyl group are detrimental, as can be observed for **9a**.

All the final compounds synthesised were also tested for their potential interference with the HCV NS3 helicase activity (Table 1). Despite the fact that **7c** shows some interference with the helicase unwinding activity at high concentrations and **3b** was found to competitively inhibit RNA binding with an IC<sub>50</sub> of 620 μM (data not shown), a trend for this effect cannot be identified, and it does not seem to correlate with any specific structural feature. Moreover, the IC<sub>50</sub> values observed are dramatically higher than the range of activities found in the HCV replicon assay, and a correlation between the two sets of data cannot be found. This evidence suggests that the antiviral effect of the pyrrolone structures presented in this study might be due to a different target, viral or cellular, other than the HCV NS3 helicase. Additional studies aimed to further explore the structure-activity relationships associated to the pyrrolone scaffold and to determine the biological target of the newly synthesised compounds are ongoing and will be reported in due course. In particular, ongoing synthetic efforts are directed to increase the water solubility of the novel antiviral scaffold, to further explore the effect of different aromatic substitutions on the 1-phenyl, 3-phenylidene and 5-phenyl rings, to evaluate the importance of the rigidity of the molecule with the preparation of unsaturated analogues, and to replace the central pyrrolone nucleus with different heterocyclic systems.

In conclusion, starting from a ligand-based *in silico* approach, a substituted pyrrolone scaffold was identified as hit for the inhibition of HCV replication in the subgenomic replicon assay. Its structure was the starting point for the design and synthesis of a first series of new analogues, with which antiviral potential was confirmed and improved. Different novel derivatives with EC<sub>50</sub> values in the low micromolar range were found. Preliminary structure-activity relationships could be identified for the antiviral effect, while the first enzymatic evaluations performed seem to suggest that the antiviral potential associated with the newly prepared compounds is not directly correlated with interference with the NS3 helicase, but other viral or cellular targets might be involved.

Further exploration of modified novel derivatives and understanding the biological target of these structures are the current focus of on-going investigations.

#### A. Supplementary material

Supplementary data associated with this article can be found, in the online version, at <http://dx.doi.org/10.1016/j.bmcl.2016.12.087>.

#### References

1. World Health Organization. Hepatitis C factsheet 164. July 2015 <<http://www.who.int/mediacentre/factsheets/fs164/en/>> [accessed November 22, 2016].
2. Marrero JA. Viral hepatitis and hepatocellular carcinoma. In: Shetty K, Wu GY, editors. Chronic viral hepatitis: diagnosis and therapeutics. 2nd ed.; 2009, p. 431–447 [Springer].
3. Suzuki T, Ishii K, Aizaki H, Wakita T. *Adv Drug Deliv Rev.* 2007;59:1200–1212.
4. U.S. Food and Drug Administration <[www.fda.gov](http://www.fda.gov)> [accessed November 22, 2016].
5. FDA approves new treatment for hepatitis C virus. Food and Drug Administration [November 22, 2013].
6. FDA approves Sovaldi for chronic hepatitis C in FDA New Release. U.S. Food and Drug Administration, 2013-12-06.
7. Rai R, Deval J. *Antiviral Res.* 2011;90:93–101.
8. Anna Suk-Fong Lok. *Clin Liver Dis.* 2013;17:111–121.
9. Gao M. *Curr Opin Virol.* 2013;3:514–520.
10. Vermehren J, Sarrazin C. *Best Pract Res Cl Ga.* 2012;26:487–503.
11. [www.gilead.com/-/media/Files/pdfs/medicines/liver-disease/harvoni/harvoni\\_pi](http://www.gilead.com/-/media/Files/pdfs/medicines/liver-disease/harvoni/harvoni_pi) [Accessed November 22, 2016].
12. Issur M, Gotte M. *Viruses.* 2014;6:4227–4241.
13. Poveda E, Wyles D, Mena A, Pedreira A, Castro-Iglesias A, Cachay E. *Antiviral Res.* 2014;108:181–191.
14. Gritsenko D, Hughes G. Lopinavir/Ritonavir (Harvoni): Improving Options for Hepatitis C virus infection. *Pharm Ther: Drug Forcast* 2015, 40, 256–259, 276.
15. Hagan LM, Sulkowski MS, Schinazi RF. *Hepatology.* 2014;60:37–45.
16. Li K, Frankowski KJ, Belon CA, et al. *J Med Chem.* 2012;55:3319–3330.
17. Lam AM, Frick DN. *J Virol.* 2006;80:404–411.
18. Kolykhov AA, Mihalik K, Feinstone SM, Rice CM. *J Virol.* 2000;74:2046–2051.
19. Tai CL, Chi WK, Chen DS, Hwang LH. *J Virol.* 1996;70:8477–8484.
20. Morris PD, Byrd AK, Tackett AJ, et al. *Biochemistry.* 2002;41:2372–2378.
21. Wilcock DJ, Lewis DW, Catlow CRA, Hutchings GJ, Thomas JM. *J Mol Catal A – Chem.* 1997;119:415–424.
22. Hawkins PCD, Skillman AG, Nicholls A. *J Med Chem.* 2007;50:74–82.
23. Daylight, Version 4.9; Daylight Chemical Information System Inc: Aliso Viejo, CA; 2008.
24. McGaughey GB, Sheridan RP, Bayly CI, et al. *J Chem Inf Model.* 2007;47:1504–1519.
25. OpenEye Scientific Software, Santa Fe, NM. <[www.eyesopen.com](http://www.eyesopen.com)> [accessed November 22, 2016].
26. Bassetto M, Leyssen P, Neyts J, Yerukhimovich MM, Frick DN, Brancale A. *Eur J Med Chem.* 2016;123:31–47.
27. Bassetto M, Leyssen P, Neyts J, et al. *Eur J Med Chem.* 2016;125:1115–1131.
28. Chen CS, Chiou CT, Chen GS, et al. *J Med Chem.* 2009;52:2716–2723.
29. Hu CY, Chen SJ, Liaw SH. *KEK Prog Rep.* 2003;2002–2002:183.

30. Specs <[www.specs.net](http://www.specs.net)> [accessed November 22, 2016].
31. Chemical Computing Group, Montreal, Canad. <[www.chemcomp.com](http://www.chemcomp.com)> [accessed November 22, 2016].
32. Chan SL, Labute P. *J Chem Inf Model*. 2010;50:1724–1735.
33. Abbandonato G, Signore G, Nifosi R, Voliani V, Bizzarri R, Beltram F. *Eur Biophys J*. 2011;40:1205–1214.
34. Bourrotte M, Schmitt M, Follenius-Wund A, Pigault C, Haiech J, Bourguignon JJ. *Tetrahedron Lett*. 2004;45:6343–6348.
35. Deo S, Inam F, Mahashabde RP, Jadhav AN. *Asian J Chem*. 2010;22:3362–3368.
36. Wang H et al. *Macromolecules*. 2011;44:4213–4221.
37. Bartensclager R. *Nature Rev Drug Disc*. 2002;1:911–916.